

Surfzone Topography-informed Deep Learning Techniques to Nearshore Bathymetry with Sparse Measurements

Yizhou Qian,¹ Hojat Ghorbanidehno,² Matthew Farthing,³
Ty Hesser,³ Peter K. Kitanidis,⁴ Eric F. Darve²

¹Institute for Computational and Mathematical Engineering, Stanford University, CA

²Department of Mechanical Engineering, Stanford University, CA

³US Army Engineer Research and Development Center, Vicksburg, MS

⁴ Department of Civil and Environmental Engineering, Stanford University, CA

¹yzqian@stanford.edu, ²{hojjatgh, darve}@stanford.edu, ³jonghyun.harry.lee@hawaii.edu,

⁴{mwfarrington, thesser1}@gmail.com, ⁵peterk@stanford.edu

Abstract

Nearshore bathymetry, the knowledge of water depth in coastal zones, has played a vital role in a wide variety of applications including shipping operations, coastal management, and risk assessment. However, direct high resolution surveys of nearshore bathymetry are relatively difficult to perform due to budget constraints and logistical restrictions. One possible approach to nearshore bathymetry without such limitations is the use of spatial interpolation with sparse measurements of water depth by using, for example, geostatistics. However, it is often difficult for traditional methods to recognize patterns with a sharp gradient often shown on coastal sand bars, especially in the case of sparse measurements. In this work, we use a conditional Generative Adversarial Neural Network (cGAN) to generate abruptly changing bathymetry samples while being consistent with our sparse, multi-scale measurements. We train our neural network based on synthetic data generated from nearshore surveys provided by the U.S. Army Corps of Engineer Field Research Facility (FRF) in Duck, North Carolina. We compare our method with Kriging on real surveys as well as ones with artificially added patterns of sharp gradient. Results show that our conditional Generative Adversarial Network provides estimates with lower root mean squared errors than Kriging in both cases.

Introduction

Nearshore bathymetry, or the topography of ocean floor in coastal zones, has been one of the most critical variables in many areas including geomorphology (Finkl, Benedet, and Andrews 2005), harbor managements (Grifoll et al. 2011) and flood risk assessment (Casas et al. 2006). Hence, accurate estimations of nearshore bathymetry with relatively low cost in area of interest, have become increasingly important in recent years due to the expansion of coastal activities and the improvement of sensor technologies. Nearshore bathymetry typically exhibits time-varying multi-scale features such as sand bars due to short-term wave and storm

forcing as well as long-term climate and sea level changes. In this work, we focus primarily on the comparisons of spatial interpolation methods (SIMs) for nearshore bathymetry. In particular, Kriging, which is one of the most widely used stochastic techniques for environmental data, will be compared with our deep learning methods.

Generative Adversarial Networks

Generative Adversarial Networks are a class of deep generative models that consists of two types of neural networks (Goodfellow et al. 2014): a generator G and a discriminator D . The generator G takes some noise vector \mathbf{z} , which is usually from some normal distribution $p_1(\mathbf{z})$, as input to generate fake images, and the discriminator takes images as input and tries to classify them as real or fake. The networks are trained in an adversarial manner: the generator G tries to generate as realistic images as possible to fool the discriminator D , while D tries to accurately distinguish between real images and fake images generated by G . Formally, let \mathbf{x} represent the bathymetric images with some prior distribution $p_2(\mathbf{x})$, then the objective function of GAN will be:

$$\min_G \max_D \mathbb{E}_{\mathbf{x} \sim p_2(\mathbf{x})} (\log D(\mathbf{x})) + \mathbb{E}_{\mathbf{z} \sim p_1(\mathbf{z})} (1 - \log D(G(\mathbf{z})))$$

Conditional Generative Adversarial Networks (cGANs) are an extension of GANs (Mirza and Osindero 2014), in which an extra label \mathbf{y} , which represents indirect observations, is passed as input to both the generator G and the discriminator D . The two networks are trained alternatively using the output of each other, and the generator will supposedly generate sample images consistent with observations at the end of several training cycles. In this work, two different scale data types of 1) point-wise sparse measurements and 2) averages over each grid are used with labels \mathbf{y} for our cGAN. The overall scheme is shown in Figure 1. The objective function of cGAN then becomes:

$$\min_G \max_D \mathbb{E}_{\mathbf{x} \sim p_2(\mathbf{x})} (\log D(\mathbf{x}|\mathbf{y})) + \mathbb{E}_{\mathbf{z} \sim p_1(\mathbf{z})} (1 - \log D(G(\mathbf{z}|\mathbf{y})))$$

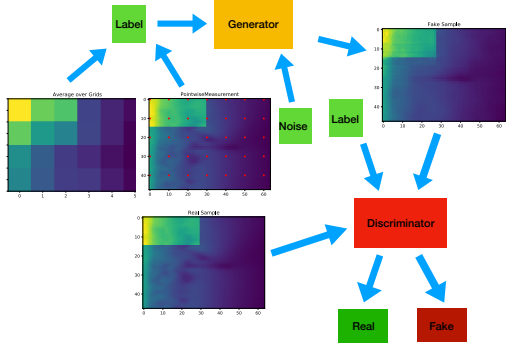


Figure 1: Conditional Generative Adversarial Network

Numerical Experiments

240 surveys are used to generate synthetic training data for cGAN by adding Gaussian noises with the following covariance matrix:

$$C_{ij} = \alpha \exp\left(-\frac{\|x_i - x_j\|^2}{r^2}\right)$$

where α is chosen in $(1, 2)$ and r is chosen in $(80, 100)$. 9600 training samples in total are generated to be training data. We also introduce random sand bar structures as our topographical understanding in the surf zone and investigate cGAN's potential ability to recognize patterns with sharp gradient. For this, rectangular jumps with random locations (uniformly in the computational domain) and random sizes are added to real bathymetry surveys (9600 samples) as well as profiles with constant values uniformly chosen from 0 to 10 (9600 samples) with Gaussian variations. We also add Gaussian white noise with a variance of 0.2 to all training input. In our comparisons below, we consider using only 35 evenly distributed grid points with a grid size of 136 meters along-shore and 76 meters across-shore for our sparse measurements. For Kriging, we used the method of CoKriging to incorporate grid cell averages as auxiliary measurements.

Performance on Real Data

In the first case, we compare cGAN with Kriging based on 15 real FRF surveys not included in the training set. For each prediction, 100 samples are generated by cGAN and we use the point-wise average over those samples as our final estimate. Figure 2 shows the root mean squared errors of cGAN and Kriging on those 15 surveys. Our results show that cGAN produces estimates of bathymetry profiles with consistently lower root mean squared errors than Kriging. This is because when training data are sampled from a carefully chosen prior distribution, deep neural networks are known to provide posterior estimates that minimize the mean squared error (Adler and Öktem 2018).

Performance on Data with

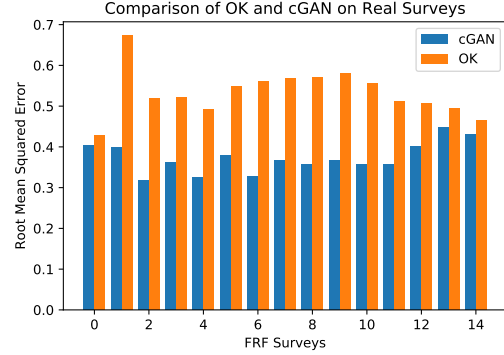


Figure 2: Comparison of Kriging and cGAN on FRF Surveys

Artificially Added Sharp Gradient

In the second case, one FRF survey taken on June 21th, 2017 is chosen for comparisons on performance of cGAN and Kriging while random rectangular jumps are added (uniformly random location and sizes). Similarly, 100 samples are generated by cGAN to compute the average as its final prediction. The result is shown in Figure 3 and Figure 4. Figure 3 shows predictions of nearshore bathymetry by cGAN and Kriging with the corresponding mean absolute error (MAE), as well as the variance of samples generated by cGAN. Figure 4 shows the corresponding cross section plots near the location of discontinuity. We observe that cGAN gives estimates with almost vertical jumps, as well as a lower mean absolute error. This is because deep neural networks can express highly complex functions in an efficient manner (Poole et al. 2016) while Kriging requires a carefully chosen nonlinear kernel function to achieve the same performance (Williams 1996). Furthermore, GAN tends to produce sharper samples than other available methods (Goodfellow 2017), thus is suitable for general nearshore bathymetry interpolation applications.

Conclusion

In this work, we compare cGAN with Kriging on real nearshore bathymetry surveys. Results show that cGAN provides estimates with lower root mean squared errors than Kriging on real FRF surveys not included in the training set. We also compared cGAN with Kriging on synthetic surveys with rectangular jumps. It is shown that cGAN produces samples with lower mean absolute errors as well as sharper boundaries.

Acknowledgement

This research was supported in part by an appointment to the Research Participation Program at the U.S. Army Engineer Research and Development Center, Coastal and Hydraulics Laboratory (ERDC-CHL) administered by the Oak Ridge Institute for Science and Education through an interagency agreement between the U.S. Department of Energy and ERDC. The research is also supported in part by

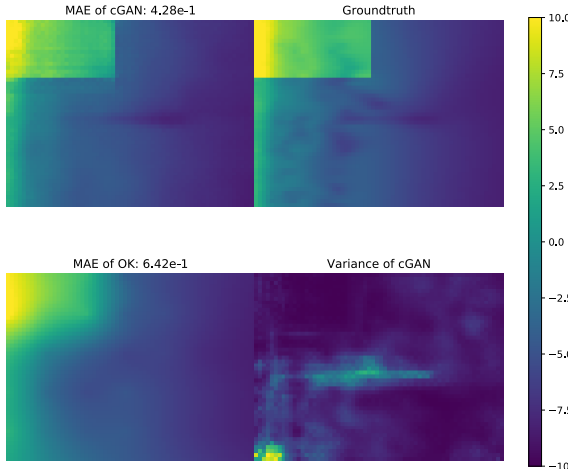


Figure 3: Performance with rectangular discontinuities. cGAN denotes conditional Generative Adversarial Network, OK denotes Kriging

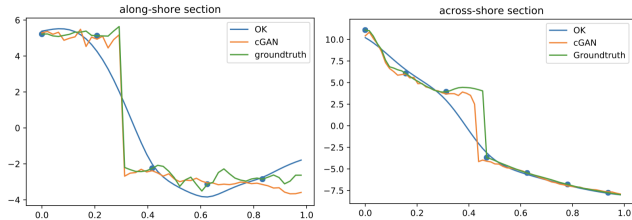


Figure 4: Cross section comparisons. cGAN denotes conditional Generative Adversarial Network, OK denotes Kriging

funding from the Army High Performance Computing Research Center (AHPCRC), sponsored by the U.S. Army Research Laboratory under contract No. W911NF-07-2-0027, at Stanford. Jonghyun Lee was supported in part by Hawai'i Experimental Program to Stimulate Competitive Research (EPSCoR) provided by the National Science Foundation Research Infrastructure Improvement (RII) Track-1: 'Ike Wai: Securing Hawai'i's Water Future Award #OIA-1557349.

References

- Adler, J., and Öktem, O. 2018. Deep bayesian inversion. *arXiv preprint arXiv:1811.05910*.
- Casas, A.; Benito, G.; Thorndycraft, V.; and Rico, M. 2006. The topographic data source of digital terrain models as a key element in the accuracy of hydraulic flood modelling. *Earth Surface Processes and Landforms* 31(4):444–456.
- Finkl, C. W.; Benedet, L.; and Andrews, J. L. 2005. Interpretation of seabed geomorphology based on spatial analysis of high-density airborne laser bathymetry. *Journal of Coastal Research* 213:501–514.
- Goodfellow, I.; Pouget-Abadie, J.; Mirza, M.; Xu, B.; Warde-Farley, D.; Ozair, S.; Courville, A.; and Bengio, Y. 2014. Generative adversarial nets. In *Advances in neural information processing systems*, 2672–2680.
- Goodfellow, I. J. 2017. NIPS 2016 tutorial: Generative adversarial networks. *CoRR* abs/1701.00160.
- Grifoll, M.; Jordà, G.; Espino, M.; Romo, J.; and García-Sotillo, M. 2011. A management system for accidental water pollution risk in a harbour: The barcelona case study. *Journal of Marine Systems* 88(1):60–73.
- Mirza, M., and Osindero, S. 2014. Conditional generative adversarial nets. *arXiv preprint arXiv:1411.1784*.
- Poole, B.; Lahiri, S.; Raghu, M.; Sohl-Dickstein, J.; and Ganguli, S. 2016. Exponential expressivity in deep neural networks through transient chaos. In Lee, D. D.; Sugiyama, M.; Luxburg, U. V.; Guyon, I.; and Garnett, R., eds., *Advances in Neural Information Processing Systems 29*. Curran Associates, Inc. 3360–3368.
- Williams, C. K. I. 1996. Computing with infinite networks. In *Proceedings of the 9th International Conference on Neural Information Processing Systems*, NIPS96, 295–301. Cambridge, MA, USA: MIT Press.